J. Phys. IV France **10** (2000)

Self-organization of shear bands in Ti, Ti-6%Al-4%V, and 304 stainless steel

V.F. Nesterenko, Q. Xue and M.A. Meyers

Department of Mechanical and Aerospace Engineering, University of California, San Diego, La Jolla, CA 92093, U.S.A.

Abstract. Adiabatic shear bands self-organize themselves: this phenomenon was investigated in three different alloys (stainless steel 304L, Ti, and Ti-6%Al-%V) through the radial collapse of a thick-walled cylinder under high-strain-rate deformation (~10^4 s^{-1}). This method was used to examine the shear-band initiation, propagation, as well as spatial distribution. The spacing of shear bands in the three materials varied widely and showed considerable differences during the initiation and propagation. Shear-band spacing is compared with the theories proposed by Grady and Kipp (momentum diffusion), Wright and Ockendon (perturbation), and Molinari (perturbation plus work hardening). Additionally, the effect of microstructural inhomogeneities on initiation is discussed. A discontinuous growth mode for shear localization under periodic perturbation is proposed based on two-dimensional growth considerations, not incorporated into the one-dimensional perturbation and momentum diffusion theories.

1. INTRODUCTION

Adiabatic shear bands occur frequently in deformation processes under high strain rates, especially in impact and penetration of projectiles, and machining operations. The spatial distribution of shear bands has been shown to exhibit periodic spacing and evolves as a self-organization phenomenon[1,2]. However, most of the past work has focused on the formation and evolution of a single shear band(SB). Grady[3], Grady and Kipp [4], Wright and Ockendon [5], and Molinari [6] gave theoretical predictions for shear band spacing that represent a beginning of our understanding of their collective behavior. Nesterenko et al. [7] developed an explosive testing method with thick-walled cylinder specimen, which was successfully used to investigate the spacing pattern of SB in titanium [2]. It was shown that the initiation of shear localization occurred by the formation of multiple shear bands, which had a spacing on the order of 0.6 mm. The purpose of this paper is to characterize the evolution of multiple SBs in different metals and to establish the underlying physics.

2. EXPERIMENTAL PROCEDURE

The experimental configuration of the thick-walled cylinder explosion technique is described in [2,7]. The specimen was sandwiched between a copper driver tube and a copper stopper tube and was collapsed inwards during the test. By varying internal diameters of the stopper and central steel rod one obtains controlled and reproducible strains.

The maximum shear strain occurs on the internal surface of the specimen, and thus shear bands initiate preferentially there. After each experiment the cylinders were sectioned and the lengths of shear bands, l_i, the edge displacements, δ_i, the average radius of final internal boundary, R_f, and the angle between spatial position from origin, Ψ_i, were measured as shown in Figure 1. The effective strain is [2]:

$$\varepsilon_{ef} = \frac{2}{\sqrt{3}}\varepsilon_{rr} = \frac{2}{\sqrt{3}}\ln\left(\frac{r_0}{r}\right) \tag{1}$$

where r_0, r_f are the initial and final radii. Based on the number of distinguishable SB, the average spacing between them is:

$$L = \frac{\Psi_i R_f}{n_i\sqrt{2}} \tag{2}$$

where n_i is the number of shear bands at the particular region i. If $n_i=n_{total}$, $\Psi_i=2\pi$.

Three different materials were selected to investigate the evolution of SB spacing: austenitic stainless steel (SS) AISI 304L (T-304L, solution treated, from 1 inch bar, $\sigma_{0.2}$=250 MPa, σ_t=640 MPa, elongation 58%) with grain size of 30 μm; commercially pure titanium (CP-Ti, Grade 2, Altemp Alloys, CA, from 2 inch bar, $\sigma_{0.2}$=360 MPa, σ_t =470 MPa, elongation 20%) with equiaxed grains having average size 20 μm; and Ti-6Al-4V alloy (MIL-T-9047G from 1 inch bar, $\sigma_{0.2}$=980 MPa, σ_t =1060 MPa, elongation 15%) with grain size of 5 μm. The high-strain-rate mechanical response was measured by means of compressive split-Hopkinson bar experiments.

3. THEORETICAL PREDICTIONS

The current theories for predicting shear band spacing can be classified into two types. They start from the one-dimensional momentum and energy conservation equations, but are correlated with different mechanisms. One is based on the concept of momentum diffusion, and was developed by Grady and Kipp (GK) [4]. The basic idea lies in the unloading from the center of the SB and is inspired by Mott's [7] fracture work. The momentum diffusion due to the unloading creates a rigid region between the shear bands. The GK model uses a simple constitutive equation, $\tau = \tau_0[1 - a(T - T_0)]$ without consideration of work hardening and strain rate effects. It is assumed that within a well-developed shear band the shear stress is reduced to zero; this corresponds to the later stages of shear localization.

The second approach uses the perturbation analysis at the critical transition from stable to unstable plastic deformation. Grady[3], and Wright and Ockendon (WO) [5] developed such an analysis for the one-dimensional simple shear case. The fastest growing perturbation wavelength associated with the instability corresponds to the minimum spacing. They selected a constitutive equation with strain-rate sensitivity and predicted the spacing of SBs. Molinari[6] modified the WO model by incorporating the effect of strain hardening into SB spacing.

In order to compare these theories, we consider the predictions without strain hardening effect. The comparison of the three theoretical models for SB spacing is shown in Table 1. The GK, WO and Molinari models have a similar form, although they were developed from different assumptions. The only difference among them is in the coefficients, which relate to the material parameters such as the strain rate hardening, m. The WO and Molinari models are the same except for a factor $[(1-aT_0)^2/(1+m)]^{1/4}$. Since m is much less than 1, this factor is approximately $(1-aT_0)^{1/2}$. For $a=1.5\times10^{-3}$, and T_0 =300K, the factor is 0.74. Thus, the Molinari as the WO predictions are on the same order. The GK model does not have a strain–rate sensitivity parameter and represents the state of affairs in the later stages of the evolution of shear localization, when shear stresses are unloaded due to thermal softening. The difference between the predictions of the GK model and WO/Molinari models is roughly 10 times for normal metals.

The GK, WO and Molinari models were compared by using the equations in Table 1, neglecting the effect of strain hardening. In the split Hopkinson bar experiments, $\dot{\gamma}_0=6\times10^4$ s^{-1}. The parameters for Ti are given in [2]. For SS [9], m=0.012; $a=7.2\times10^{-4}$ K^{-1}; k=14.7 J/smK; C=500 J/kgK; τ_0=200 MPa. For Ti-6Al-4V [9,10], m=0.024; $a=2\times10^{-3}K^{-1}$; k=3.07 J/smK; C=564 J/kgK; τ_0=490 MPa. These shear-band spacings are on the order of 0.01-0.2 mm for the WO/M theories. On the other hand, the Grady's predictions vary between 1 and 3 mm.

4. EXPERIMENTAL RESULTS

Nesterenko et al.[2] concluded, for titanium, that the WO/M theory provided a good description of the initiation of shear localization, whereas Grady's theory described better the propagation stage. These results are reanalyzed here.

The patterns of shear bands in SS, Ti and Ti-6Al-4V alloy exhibit different characteristics during their evolution. Figure 2 shows, in schematic fashion, the distribution of shear bands for the different materials. Only a small fraction of the bands are shown. The number of bands is marked in the bottom of

Table 1 Theoretical Predictions of Shear Band Spacing For Three Materials

	Grady-Kipp	Wright-Ockendon	Molinari (n=0, Without Strain Hardening)
Spacing	$2\pi\left[\frac{kC}{\dot{\gamma}_0^3 a^2 \tau_0}\right]^{1/4} \cdot \frac{9^{1/4}}{\pi}$	$2\pi\left[\frac{kC}{\dot{\gamma}_0^3 a^2 \tau_0}\right]^{1/4} \cdot m^{3/4}$	$2\pi\left[\frac{kC}{\dot{\gamma}_0^3 \tau_0 a^2}\right]^{1/4} \cdot \left[\frac{m^3(1-aT_0)^2}{(1+m)}\right]^{1/4}$
SS 304L	**2.62**	**0.17**	**0.16**
CP Titanium	**3.3**	**0.52**	**0.36**
Ti-6Al-4V	**0.876**	**0.094**	**0.085**

each schematic. For 304 SS, the distinguishable number in the initial stage (ε_{ef}=0.55) is 235, corresponding to a spacing L_i=0.12 mm. The number of the active SBs in the later stages significantly decreases with the increase in effective global strain; in this "Darwinian" system, many shear bands are initiated but only a few (the fittest!) continue growing. For Ti, the number of bands is approximately 100 (L_i=0.18mm).This spacing is considerably lower than the one reported by Nesterenko et al.[2](0.6 mm) because a closer examination of the results revealed large populations of incipient bands that did not grow. In a similar manner to 304 SS, only a fraction of the bands grow, in the later stages of deformation. For Ti-6Al-4V alloy, SB patterns were examined at four different effective global strains: 0.13, 0.26, 0.55, and 0.92(Figure 2). At the higher strains, the number of shear bands is almost keeps the same (approximately 66); the SB patterns at highest two strains become chaotic. Even at the low strain level (0.26), the SBs are well-developed and propagate large distances into the material bulk. The corresponding spacing of SBs is L_i=0.526 mm. The SB pattern at smaller strain (0.13) in Ti-6Al-4V was also monitored to find the initial state of SBs. The average spacing is about 1.12 mm and the general picture does not reveal periodicity. If one compares these results with the predictions in Table 1, one has to conclude that the significant differences encountered are not theoretically predicted. The large spacing in Ti-6Al-4V in comparison with SS and Ti cannot be explained by the present theories. This significant difference is illustrated in Figure 3. In fact, the theories predict an opposite effect.

A better quantitative assessment of shear-band evolution is provided by plotting their lengths, L_i, as a function of position. This is done in Figure 3 for AISI 304 stainless steel and for Ti-6%Al-4%V. These plots were made at two levels of global strain. It can be seen that (a) the number of shear bands at the early stages is much larger for SS than for Ti6Al4V, and (b) at the late stages, only a fraction of the shear bands grow. The numbers given in the bottoms of the schematics shown in Fig. 2 do not reveal these differences, since they are total values (small + large).

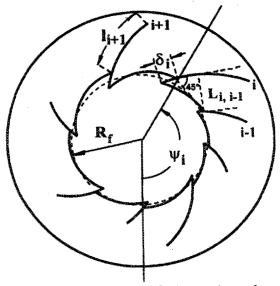

Figure 1. Characteristics of shear band pattern

The results suggest that the interaction between nuclei of SBs in Ti-6Al-4V is relatively weak. Each shear band grows fast once it nucleates. Unloading from the developed SB during growth reduces the new nucleation sites in the surrounding areas. The examination of the ratio of the lengths of SBs and their edge displacement, L/δ, also indicates the difference between SS and Ti-6Al-4V. Figure 4 shows the initial stage of shear band in SS and Ti-6Al-4V with the same edge length δ. The same δ means that the local shear strains at the root of single SB are the same. L/δ is about 9.5 for stainless steel and 26.5 for Ti-6Al-4V at the same δ. This result suggests that the SB develop much faster in Ti alloy than in SS.

The WO/M models, based on perturbation analysis, reflect the initial behavior of shear bands. These predictions may correlate to the initial spacing. The GK model considers the extreme case in which the shear band totally loses its capacity to resist load. If we consider critical cut-off lengths for the SBs(e.g., 2.5 mm for SS and 2.62 mm for Ti), the new spacings are 3.2 and 2.57 mm for SS and titanium,

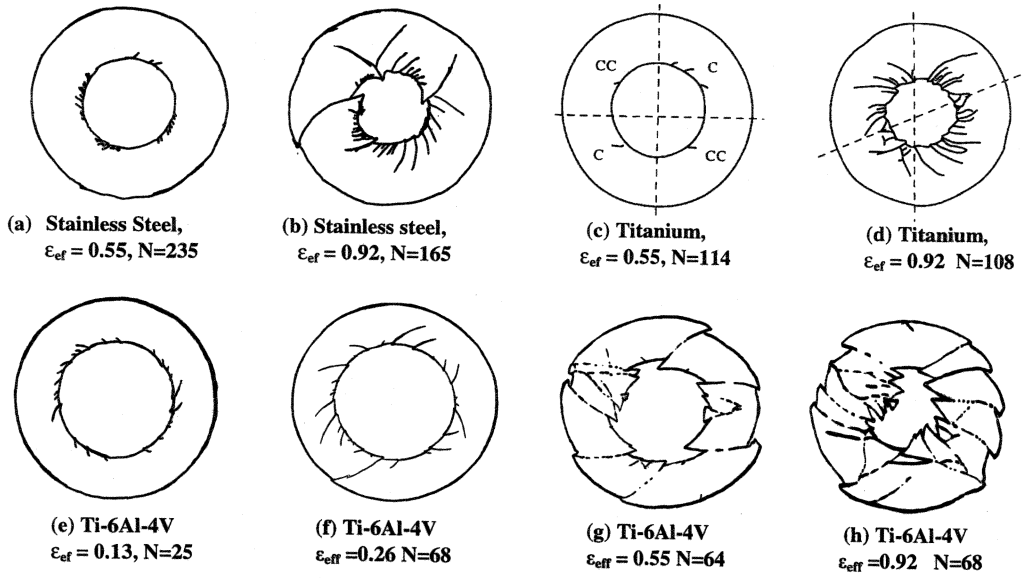

(a) **Stainless Steel,** $\varepsilon_{ef} = 0.55$, N=235

(b) **Stainless steel,** $\varepsilon_{ef} = 0.92$, N=165

(c) **Titanium,** $\varepsilon_{ef} = 0.55$, N=114

(d) **Titanium,** $\varepsilon_{ef} = 0.92$ N=108

(e) **Ti-6Al-4V** $\varepsilon_{ef} = 0.13$, N=25

(f) **Ti-6Al-4V** $\varepsilon_{eff} = 0.26$ N=68

(g) **Ti-6Al-4V** $\varepsilon_{eff} = 0.55$ N=64

(h) **Ti-6Al-4V** $\varepsilon_{eff} = 0.92$ N=68

Figure 2. Evolution of shear band pattern in stainless steel(a,b); titanium(c,d); and Ti-6Al-4V alloy (e-g).

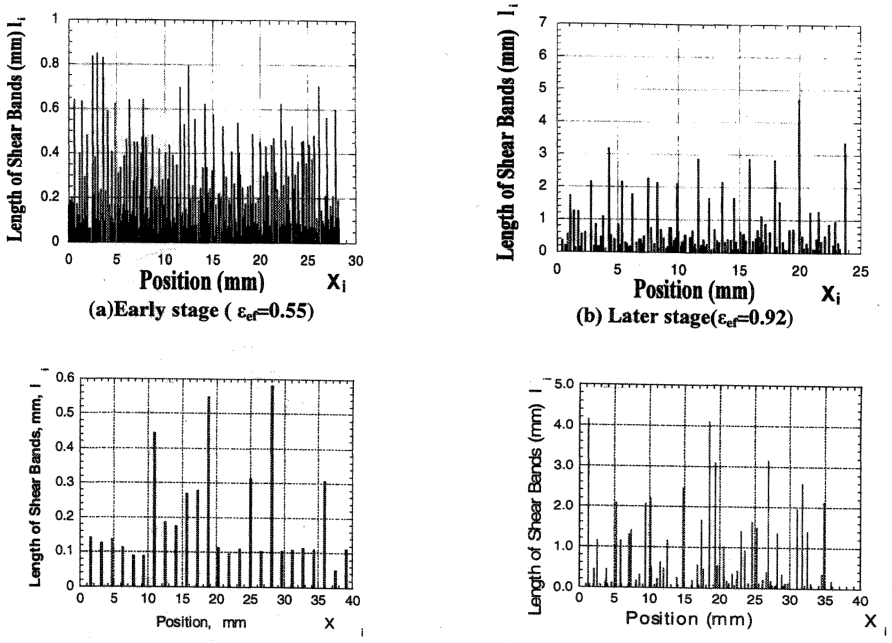

(a)Early stage (ε_{ef}=0.55)

(b) Later stage(ε_{ef}=0.92)

(c) **Initial stage** ($\varepsilon_{ef} = 0.13$)

(d) **Later stage** ($\varepsilon_{ef} = 0.26$)

Figure 3. Shear band distribution in (a,b) 304 SS and (c,d) Ti-6%Al-4%V at different stages.

respectively. These results are fairly close to the predicted GK values, 2.62 and 3.3 mm. However, these theories cannot account for the large differences in spacing observed in the current experiments. Therefore, they can only be considered as a first approximation to the spacing of shear bands.

5. ADDITIONAL (TWO DIMENSIONAL) CONSIDERATIONS

The current experimental results for AISI 304 stainless steel and Ti-6%Al-4%V seem to corroborate

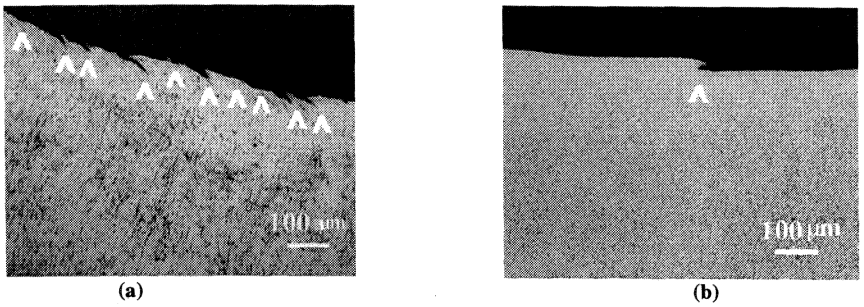

(a) (b)

Figure 4. Comparison of spacings for stainless steel(a) and Ti-6Al-4V alloy(b) at initial stage.

the initial, preliminary conclusions of Nesterenko et al.[2]. However, a closer examination of the experimental results reveals that the shear-band interactions are more complex, and that other factors seem to play an important role. Three important factors determine shear-band spacing:

a) Rate of nucleation of shear bands. The probability of nucleation, $P(V_0)$, in a reference volume, V_0, can be described by a Weibull distribution , using strain as the independent variable (in lieu of stress, in the conventional approach). Thus, it is equal to:

$$P(V_0)=1-\exp\{-[(\varepsilon-\varepsilon_i)/\varepsilon_0]^q\} \quad (3)$$

where ε_i, is the critical strain below which no initiation takes place, ε_0 is a material constant, and, ε is the variable , and q is a Weibull modulus. The rate of nucleation can be obtained by taking the time derivative of the above expression.

b) Rate of growth (or growth velocity). The velocity of SBs, relative to unloading, is an important factor that affects their spatial distribution, an aspect which the current theories have not covered. The driving force for shear-band propagation is the elastic energy release. Thus, growth is governed by stress, whereas initiation is governed by strain. The necessary condition is:

$$\tau_g<\tau_i \quad (4)$$

where τ_g and τ_i are the critical shear stresses for growth and initiation, respectively. The greater the difference, the higher the velocity of propagation.

c) Rate of deformation of specimen. It is expressed through the strain rate.

d) The interactions among shear bands can only be treated as one-dimensional events at the simplest, elementary level. The volume of material shielded from further nucleation and growth increases with the length of a shear band and is not constant, as predicted by the one-dimensional GK theory.

With these elements in place, one can construct a more realistic two-dimensional theory for the evolution of the self-organization of shear bands; this is in progress[12]. These elements are incorporated, at a preliminary stage, into the diagram of Figure 5, which depicts the evolution of shear-band spacing. Different evolution stages are schematically indicated in Figure 5(a). The evolution of shear band spacing passes through several stages: random nucleation(t_1); self organization into "periodic" pattern among nuclei (t_2); faster growth of favorable shear bands suppressing others (t_3); self organization of developed shear bands (t_4). There is a clear increase in the spacing of the propagating SBs for SS and Ti as their lengths increase. This phenomenon is analogous to the increasing spacing of propagating parallel cracks studied by Nemat-Nasser et al. [13]. At a certain length l_i, the spacing is L_i; the growth becomes unstable at a critical length $l_{cr,i}$, and alternate SBs grow with a new spacing L_{i+1}; the other shear bands stop growing. The mathematical re-presentation of the step function shown in Fig. 5b is

$$L = L_0 + \sum_{j=1}^{n} k_j' \cdot H\left(l - l_{cr,j}\right) \quad (5)$$

where $H(l-l_{cr,i})$ is a Heaviside function. The parameters k_j' can be expressed as:

$$k_j'=f(v, L_0, \varepsilon_i, \varepsilon_p) \quad (6)$$

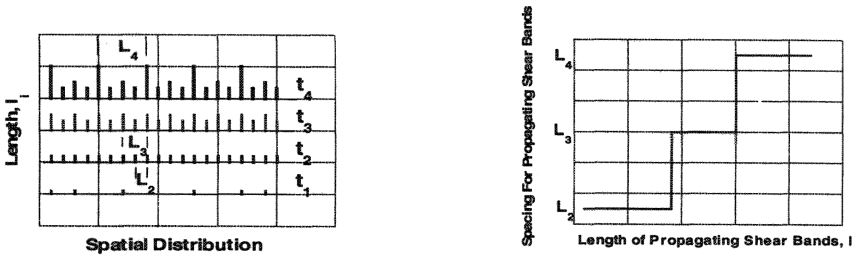

(a) (b)

Figure 5. (a) Schematic diagram of the evolution of shear band spacing at different levels. T_1-random initiation; t_2-self organization into "periodic" pattern among nuclei; t_3-some shear bands grow faster suppressing others; t_4-self organization of developed shear bands. (b) spacing of propagating SBs as a function of length.

where v is the shear band propagation velocity, L_0 is the initial spacing, ε_i, is the critical strain for initiation and ε_p is the critical strain for propagation.

It should be mentioned that Ti-6Al-4V is missing stage t_2 where the nuclei are organized in a periodic pattern with a characteristic spacing. Instead, stage t_1 with random nucleus spacing, develops into stages t_3 and t_4, bypassing t_2. This can be owe to a low value of q in Eqn. 3, i.e. abroad range of strains over which the Sbs nucleate. The difference in L/δ ratio reflects the difference between critical strains for initiation and propagation and in speed of SB development in SS and Ti-6Al-4V.

6. CONCLUSIONS

Shear band spacings in Ti, SS, and Ti-6Al-4V were experimentally measured and are shown to evolve during the deformation process. Comparison with analytical predictions shows that the WO /M model predicts the initial level of self organization of shear bands, while the GK model shows a better agreement with the behavior at the developed stage of shear bands. Nevertheless, these theories do not predict the significant differences observed. A discontinuous growth mode is proposed, wherein the spacing changes periodically, when the spacing reaches the interaction distance between adjacent shear bands, which is a function of their lengths. Chaotic versus self-organized initiation and propagation modes are discussed in a preliminary fashion from growth of some favorable shear bands.

Acknowledgments: This work was supported by U.S.A. Army Research Office under MURI program No. DAAH004-96-1-0376 (Program Manager David Stepp). Discussions with and support by Dr. T. W. Wright are greatly appreciated. Prof. V. Lubarda's and Dr. D. Curran's help are gratefully acknowledged.

REFERENCES

[1] Bai, Y. and Dodd, B., *Adiabatic Shear Localization*, Pergamon, Oxford, 1992 pp.24-44
[2] Nesterenko, V.F., Meyers, M.A., and Wright, T.W., *Acta Mat.*, **46**, 327-340 (1998).
[3] Grady,D., *J. Geoph. Res.*, **85**,913-924(1980).
[4] Grady, D.E., and Kipp, M.E., *J. Mech. Phys. Solids,* **35**, 95-118 (1987).
[5] Wright, T.W., and Ockendon, H., *Int. Journal of Plasticity*, **12**, 927-34 (1996).
[6] Molinari, A., *J. Mech. Phys. Sol.* **45**, 1551-75(1997).
[7] Nesterenko, V.F., Bondar, M.P., *DYMAT Journal*, **1**, 245- (1994).
[8] Mott,N. F., *Proc. Roy. Soc.*,**189,** 300 (1947)
[9] Stout, M.G., Follansbee, P.S., *Trans. ASME., J of Eng Mat. & Tech*, **108**, 344-53 (1986).
[10] Nemat-Nasser, S., Guo, W., Nesterenko, V.F., Indrakanti, S.S., and Gu, Y., (in press) (1999).
[11] Donachie, M.J. JR., Titanium and Titanium Alloys, ASM Press, Metal Park, 1982, pp.3-19.
[12] Xue, Q., Nesterenko, V. F., and Meyers, M. A., unpublished results(2000).
[13] Nemat-Nasser, S., and Keer L.M. and Parihar, K.S., Int. J. Solids Structures, **14**, 409-430 (1978).